

This work was written as part of one of the author's official duties as an Employee of the United States Government and is therefore a work of the United States Government. In accordance with 17 U.S.C. 105, no copyright protection is available for such works under U.S. Law.

Public Domain Mark 1.0

<https://creativecommons.org/publicdomain/mark/1.0/>

Access to this work was provided by the University of Maryland, Baltimore County (UMBC) ScholarWorks@UMBC digital repository on the Maryland Shared Open Access (MD-SOAR) platform.

Please provide feedback

Please support the ScholarWorks@UMBC repository by emailing scholarworks-group@umbc.edu and telling us what having access to this work means to you and why it's important to you. Thank you.

RESEARCH ARTICLE

10.1002/2016JD024998

Key Points:

- These measurements represent the first open ocean satellite validation using the Pandora
- Satellite measurements overestimate NO₂ and O₃ over the open ocean during this study
- Boundary layer heights using total column and surface measurements of NO₂ disagree with modeled and satellite-derived boundary layer heights

Correspondence to:

D. K. Martins,
douglas.martins@flir.com

Citation:

Martins, D. K., R. G. Najjar, M. Tzortziou, N. Abuhassan, A. M. Thompson, and D. E. Kollonige (2016), Spatial and temporal variability of ground and satellite column measurements of NO₂ and O₃ over the Atlantic Ocean during the Deposition of Atmospheric Nitrogen to Coastal Ecosystems Experiment, *J. Geophys. Res. Atmos.*, 121, 14,175–14,187, doi:10.1002/2016JD024998.

Received 25 FEB 2016

Accepted 20 OCT 2016

Accepted article online 23 OCT 2016

Published online 5 DEC 2016

Spatial and temporal variability of ground and satellite column measurements of NO₂ and O₃ over the Atlantic Ocean during the Deposition of Atmospheric Nitrogen to Coastal Ecosystems Experiment

Douglas K. Martins^{1,2}, Raymond G. Najjar¹, Maria Tzortziou³, Nader Abuhassan^{4,5}, Anne M. Thompson⁴, and Debra E. Kollonige⁶
¹Department of Meteorology and Atmospheric Sciences, The Pennsylvania State University, University Park, Pennsylvania, USA, ²Now at FLIR Detection, Inc, West Lafayette, Indiana, USA, ³Department of Earth and Atmospheric Science, City University of New York, New York, New York, USA, ⁴NASA Goddard Space Flight Center, Greenbelt, Maryland, USA, ⁵Joint Center for Earth Sciences Technology, University of Maryland, Baltimore County, Baltimore, Maryland, USA, ⁶Earth System Science Interdisciplinary Center, University of Maryland, College Park, Maryland, USA

Abstract In situ measurements of O₃ and nitrogen oxides (NO + NO₂ = NO_x) and remote sensing measurements of total column NO₂ and O₃ were collected on a ship in the North Atlantic Ocean as part of the Deposition of Atmospheric Nitrogen to Coastal Ecosystems (DANCE) campaign in July–August 2014, ~100 km east of the mid-Atlantic United States. Relatively clean conditions for both surface in situ mixing ratio and total column O₃ and NO₂ measurements were observed throughout the campaign. Increased surface and column NO₂ and O₃ amounts were observed when a terrestrial air mass was advected over the study region. Relative to ship-based total column measurements using a Pandora over the entire study, satellite measurements overestimated total column NO₂ under these relatively clean atmospheric conditions over offshore waters by an average of 16%. Differences are most likely due to proximity, or lack thereof, to surface emissions; spatial averaging due to the field of view of the satellite instrument; and the lack of sensitivity of satellite measurements to the surface concentrations of pollutants. Total column O₃ measurements from the shipboard Pandora showed good correlation with the satellite measurements ($r = 0.96$), but satellite measurements were 3% systematically higher than the ship measurements, in agreement with previous studies. Derived values of boundary layer height using the surface in situ and total column measurements of NO₂ are much lower than modeled and satellite-retrieved boundary layer heights, which highlight the differences in the vertical distribution between terrestrial and marine environments.

1. Introduction

Over the past two decades, air quality regulations have created controls that have resulted in a decrease in air pollutant concentrations such as ozone (O₃) and nitrogen dioxide (NO₂) over the United States. On average, O₃ and NO₂ have decreased 28% and 58%, respectively, from 1980 to 2010 [United States Environmental Protection Agency, 2012]. Regions of nonattainment in some areas are increasing in size, in part due to the more stringent air quality standards [U.S. EPA 2012; Duncan et al., 2016]. The nonattainment areas are defined, in part, using observational data collected by in situ, ground-based networks. These networks are labor intensive and expensive to operate; thus, the density of measurements can be less than ideal to capture the spatial variability of pollutants. High-frequency remote sensing measurements of atmospheric pollutants from ground-based networks of automated sensors such as Pandora are useful to assess spatial and temporal dynamics of atmospheric pollution and evaluate impacts of controls on air quality [Herman et al., 2009; Tzortziou et al., 2015].

Satellite measurements have been providing global coverage of air pollutants since the early 1980s [e.g., Fishman et al., 2008 and references therein]. The most recent measurements are from a suite of satellites called the “A-Train,” which consists of seven Sun-synchronous, polar-orbiting satellites. These measurements have been used in air quality forecasting, process-based studies, model development, source attribution, and emissions inventory development over the past four decades [e.g., Fishman et al., 2008 and references therein].

A challenge for satellite measurements is obtaining information on air quality near the surface [National Research Council, 2008]. The relatively coarse spatial resolution of satellite sensors (e.g., 13 km \times 24 km at nadir of the Ozone Monitoring Instrument, OMI) is not adequate for urban-scale mapping. Interferences in the upper layers of the atmosphere caused by particles and clouds act to increase molecular scattering and decrease the signal-to-noise ratios detected by the satellites, ultimately decreasing the amount of information from the troposphere and the near surface that reaches the satellite.

Recently, Duncan *et al.* [2016] used 0.1° \times 0.1° spatial resolution OMI NO₂ data to examine trends in urban regions globally over the period 2005–2014. OMI NO₂ are typically lower compared to ground-based column measurements in urban environments and higher in rural environments [Lamsal *et al.*, 2014]. These differences highlight the impact that differences in fields of view of ground-based versus satellite measurements can have on column retrievals. Knepp *et al.* [2015] and D. E. Kollonige *et al.* (Estimating surface nitrogen dioxide over South Africa from remotely-sensed total-column observations, submitted to *Remote Sensing of Environment*, August 13, 2015, hereinafter referred to as Kollonige *et al.*, submitted manuscript, 2015) demonstrated that Pandora spectrometric column NO₂ observations at suburban-to-urban stations can be used to derive a reasonable estimate of surface NO₂. They estimated surface NO₂ in a similar manner from OMI overpass columns and found good (15–20%) agreement with the Pandora-based surface estimates. These new data have heightened interest in the evaluation of OMI NO₂ retrievals, especially in the use of instruments like Pandora, and in further comparisons of in situ and column-based surface NO₂ mixing ratios. These techniques rely on measurements of the boundary layer height and assumptions regarding the shape of the NO₂ vertical profile. Over continental urban regions, the NO₂ column amount below 1 km is greater than 65% of the total column. In remote continental regions and remote oceans, NO₂ column amounts below 1 km are less than 60% and less than 3% of the total column, respectively [Velders *et al.*, 2001].

The OMI column NO₂ and O₃ retrievals have been extensively evaluated using aircraft-based [e.g., Boersma *et al.*, 2008] and balloon-based in situ measurements [e.g., Osterman *et al.*, 2008], as well as ground-based remote sensors [e.g., McPeters *et al.*, 2008]. Ground-based remote sensors, such as the Dobson, Brewer, and Pandora spectrometers are particularly useful in that the data retrievals employ some of the same analytical approaches and processing analyses used in satellite retrievals. The use of the direct-Sun Pandora, along with its spectral-fitting algorithms, avoids assumptions of stationarity, horizontal homogeneity (i.e., spatial averaging of urban and rural environments), and NO₂ profile shape associated with zenith or multiaxis differential optical absorption spectroscopy (DOAS) [Herman *et al.*, 2009]. Comparisons between Pandora total column NO₂ (TCNO₂) and the OMI NO₂ total column (level 2, version 3) show good agreement, especially during clear sky irradiances, and Pandora has higher precision during periods with partly cloudy days compared to the Brewer [Cede *et al.*, 2006; Tzortziou *et al.*, 2015]. A correlation coefficient (*r*) of 0.73 (slope = 0.98) was observed between Pandora and OMI over 2 years at the NASA Goddard Space Flight Center (Greenbelt, MD), which is an urban environment [Herman *et al.*, 2009]. Pandora total column ozone (TCO₃) and a well-calibrated double-grating Brewer spectrometer showed good agreement over a period of more than a year in Greenbelt, MD, with Pandora TCO₃ approximately 2 Dobson units (DU) or 0.6% higher compared to the Brewer [Tzortziou *et al.*, 2012]. This difference was constant with slant column ozone amount over the full range of observed solar zenith angles (SZAs, 15–80°), indicating adequate Pandora stray light correction. Pandora TCNO₂ and TCO₃ measurements were extensively compared with Aura-OMI retrievals during NASA's Deriving Information on Surface Conditions from Column and Vertically Resolved Observations Relevant to Air Quality (DISCOVER-AQ) July 2011 field campaign in the Baltimore, MD/Washington, DC, region [Lamsal *et al.*, 2014; Tzortziou *et al.*, 2015; Reed *et al.*, 2015]. These comparisons showed that TCNO₂ retrieved from OMI was on average 15% lower than that from Pandora. Total column ozone retrievals were in very good agreement, with OMI retrieving 3% higher TCO₃ than Pandora. These studies also showed that the agreement between OMI and Pandora is typically improved when the cross-track position of the Aura satellite carrying OMI is less than 50 km from the Pandora location and the cloud fraction is <0.2.

Information on TCNO₂ and TCO₃ in offshore waters remains extremely scarce. Air quality measurements over the ocean are important because they provide insights into environments that are conducive to atmospheric deposition and important sources of nitrogen, iron, and other elements that influence marine planktonic ecosystems [Reay *et al.*, 2008]. In addition, satellite measurements and model simulations over marine environments are often used as initial and background conditions for regional and global chemical transport

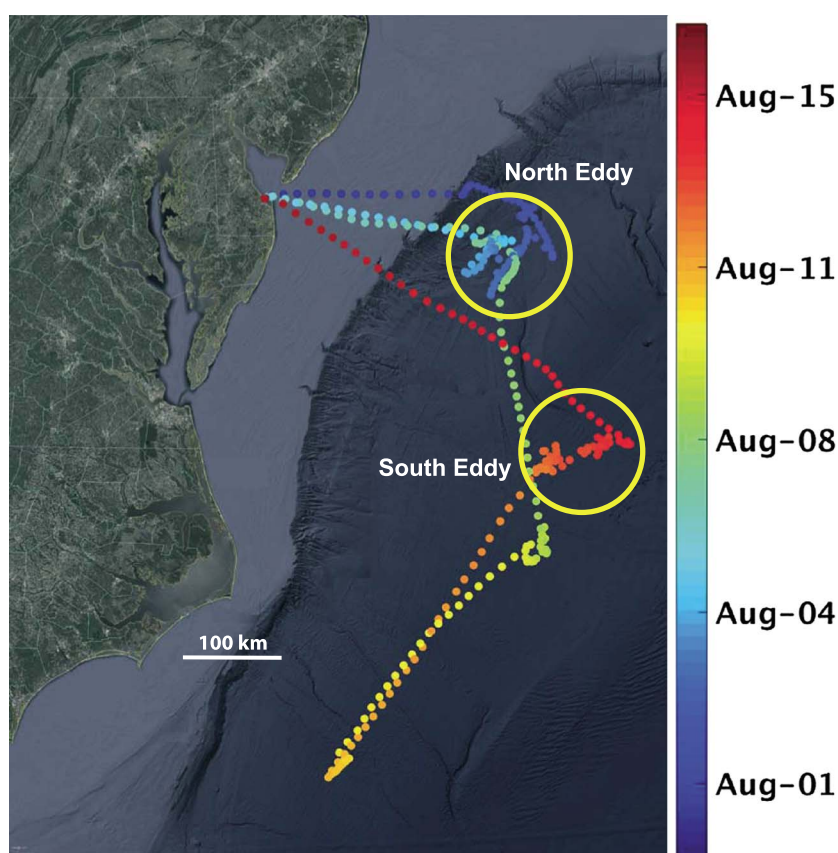


Figure 1. Ship track with time indicated by color. The approximate locations of the north and south eddies are shown (yellow circles).

models. Thus, it is important to understand the biases and uncertainties of these model inputs. Recent measurements show that diurnal and weekly patterns can be observed in TCNO₂ over a major urban estuary [Tzortziou *et al.*, 2014], but these measurements do not extend farther into offshore waters to show the impact that urban emissions have on TCNO₂.

In this manuscript, we present results from measurements collected as part of the Deposition of Atmospheric Nitrogen to Coastal Ecosystems (DANCE) cruise in the North Atlantic Ocean during the summer of 2014. This work represents the first open ocean evaluation of satellite measurements using the ship-based, direct-Sun Pandora spectrometer. We discuss the temporal and spatial variability of TCNO₂ and TCO₃. We compare the Pandora TCNO₂ and TCO₃ measurements with coincident and colocated in situ surface measurements and satellite measurements from OMI. Finally, we derive marine boundary layer heights using the coincident total column NO₂ from Pandora and in situ NO₂ surface mixing ratios.

2. Methods

2.1. Platform and In Situ Measurements

Air quality and meteorological measurements were collected on board the Research Vessel *Hugh R. Sharp* operated by the University of Delaware from 29 July to 15 August 2014. The ship embarked from Lewes, DE (38.7886 N; 75.1615 W) and targeted a semipermanent, oceanic, anticyclonic eddy (here referred to as the north eddy; ~38.35 N; 72.56 W; Figure 1). These eddies were sampled for other purposes than the work presented here. The ship returned to port on 5 August due to weather and scheduled maintenance, completing the first leg of the campaign. The ship embarked on the second leg of the campaign toward the north eddy and sampled there through 7 August and then steamed southward toward a second anticyclonic eddy (referred to as the south eddy; ~35.64 N; 72.16 W). On 10 August, the ship steamed to the southwest to

intercept rain and then returned to the south eddy by 12 August. The south eddy was sampled until midday on 14 August, when the ship returned to port, completing the second leg of the campaign.

On board, measurements of O_3 (Thermo Scientific 49C) and NO_2 (Aerodyne CAPS NO_2) were collected. The CAPS NO_2 instrument was calibrated in the laboratory prior to and after the ship deployment using a commercially available standard gas (Praxair, Inc.) with an uncertainty of 5%. An O_3 -generating ambient monitoring calibration system (EnviroNics EN-9100) traceable to a National Institute of Standards and Technology primary standard for O_3 with an uncertainty of 3% was used to calibrate the O_3 analyzer. Analyzer responses between prior and post deployment calibrations were less than 1%. The analyzers were secured in the dry laboratory with 6 m of inlet (0.17 inch ID) mounted to the port side, 9 m forward and 5 m below the ship exhaust stack. The inlet was 5 m above the water, pointed aft, and with a funnel on the end to avoid sea spray. The inlets were insulated inside the climate-controlled laboratory, the most likely section of line for condensation to occur. The inlets were inspected daily for water accumulation, and no visible water was observed.

In situ surface measurements influenced by the ship's exhaust plume were removed. The placement of the inlet was limited by the strength of each instrument's pump pulling through the 0.17 inch ID tubing. The placement of the inlet was forward of the ship's exhaust stack, on the port side, behind the bridge. When the relative wind direction was coming across the bridge, it created a partial vacuum on the lee side near the inlet, pulling the ship's exhaust forward toward the inlet. This artifact was diagnosed by observing spikes in the NO measurement, coupled with NO_2/NO ratios of <2 when the wind direction relative to the ship was from 0 to 90. Low NO_2/NO ratios are indicative of fresh or unaged emissions, since NO is the primary pollutant and most NO_2 is produced through photochemical oxidation of NO . Additionally, relative wind directions from 90 to 200 were removed because of influences from the ship. Thus, the only filter applied to the data was the relative wind direction. Influences from the ship plume were observed on 56% of the measurements, and these data were removed prior to subsequent analyses.

2.2. Pandora System

A ship-based, direct-Sun Pandora spectrometer (Pandora) [Herman *et al.*, 2009] was used to measure $TCNO_2$ and TCO_3 . Pandora collects direct sunlight using an optical head sensor with neutral density filters and two ultraviolet band pass filters (BP300, 280–320 nm) and U340 (280–380 nm). The light is passed from the head sensor to a spectrometer (Avantes) using a fused silica optical fiber. The spectrometer has a UV-sensitive, back-thinned 2048×64 pixel charge-coupled device. The spectrometer is temperature controlled using an actively coupled thermoelectric cooler and heater. The head sensor is mounted on two computer-controlled motors to control the azimuth and zenith viewing angles to $\pm 0.01^\circ$. A camera mounted in the head sensor detects the motion of the Sun due to changes in the ship's attitude and time of day. Software then utilizes the information from the camera to adjust the motors to maintain a direct-Sun viewing angle. The Pandora was mounted on top of the bridge, ~10 m forward of the ship's smokestacks and engine exhaust to avoid sample contamination.

The Pandora data were filtered following Tzortziou *et al.* [2015] for a normalized root-mean-square of the weighted spectral fittings of <0.05 , SZAs $<70^\circ$, and the uncertainties were 0.05 and 2 DU for NO_2 column and O_3 measurements, respectively. The number of valid column measurements collected over the sample period was 3180 (65% of total measurements) and 3793 (84% of total measurements) for O_3 and NO_2 , respectively. Valid data were collected on 16 out of 17 days of the campaign. The Pandora TCO_3 and $TCNO_2$ were binned based on the relative wind direction of the ship to diagnose if the measurements were impacted by the ship's exhaust plume. Inspecting the interquartile ranges of each bin shows no significant difference between the bins. Thus, we do not expect any significant influence from our own ship's plume. The separation of the stratosphere from the troposphere was not available in these Pandora measurements, so the total column measurements are used in this study.

Previous comparisons between Pandora and a well-calibrated double-grating Brewer spectrometer characterized by a very low internal stray light fraction at the short UV-B wavelengths ($<10^{-7}$ m) showed good agreement (differences within $\pm 3\%$, and a bias of 0.6%) over a wide range of SZAs ($15\text{--}80^\circ$) (i.e., up to slant column ozone amounts of 1500 DU). The practically negligible SZA dependence of the TCO_3 residuals showed that the stray light correction method applied to Pandora provides an adequate correction [Tzortziou *et al.*, 2012, 2015]. A small (1–2%) seasonal difference was found in previous studies [Tzortziou *et al.*, 2012], consistent with sensitivity studies showing that the Pandora spectral fitting TCO_3 retrieval has

a temperature dependence of 1% per 3 K, with an underestimation in temperature resulting in an underestimation of TCO₃ (e.g., during summer).

2.3. OMI Data

Total column NO₂ and O₃, level 2 swath data from the OMI on board the Aura spacecraft were used for this study (OMNO2 and OMTO3, version 3, 10.5067/Aura/OMI/DATA2017) [Bucsela *et al.*, 2013]. Aura is a Sun-synchronous, polar-orbiting satellite with an orbital period of 99 min and an overpass at a given point on the Earth's surface once per day at approximately 13:30 (local standard time (LST)). OMI conducts 60 cross-track field-of-view (FOV) scans 2600 km wide with a ground spatial resolution of 13 × 24 km at nadir. The meridional size of an OMI pixel varies with cross-track viewing zenith angle from 24 km in the nadir to ~128 km for the extreme viewing angles of 57° at the edges of the swath [Boersma *et al.*, 2007].

Total column NO₂ is retrieved using UV-Visible spectra ranging from 270 to 500 nm. Slant columns of NO₂ are calculated using a differential optical absorption spectroscopy (DOAS) fitting algorithm [Platt and Stutz, 2008]. A background vertical column density (VCD) is calculated at lower spatial resolution (1° × 1°) from 12 h of orbital data, excluding areas of persistently high NO₂ columns (i.e., metropolitan areas). Individual FOV measurements are compared with the background VCD, and the difference is scaled by the ratio of background and polluted air mass factors (AMF), resulting in the final NO₂ total VCD.

The OMI data were filtered using the quality flag for O₃ and the AMF, tropospheric vertical column, cross-track, and master quality flags for NO₂. The data were filtered to only include measurements with cloud fractions < 0.2.

2.4. Other Tools

Ensemble trajectory analyses from the Hybrid Single Particle Lagrangian Integrated Trajectory Model (HYSPLIT) were run backward for 48 h from the location of interest using North American Mesoscale (NAM) Forecast System 12 km meteorological simulations [Stein *et al.*, 2015]. Trajectories of air parcels reaching 500 m, 2000 m, and 5000 m above the surface were considered.

Boundary layer heights were estimated from Pandora and in situ measurements of total column and surface NO₂ mixing ratios, respectively, using methods described in previous studies [Knepp *et al.*, 2015; Kollonige *et al.*, submitted manuscript, 2015]. These methods assume that surface emissions are well mixed with the planetary boundary layer as a first-order approximation and that most of the NO₂ in the troposphere is within this layer.

3. Results and Discussion

3.1. Surface Measurements

Median surface NO₂ mixing ratios of 3.3 ppbv (25th percentile, 2.1 ppbv; 75th percentile, 4.3 ppbv) were observed (Figure 2a). These mixing ratios are similar to regional boundary layer medians along the east coast but lower than mixing ratios observed in an urban plume along the East Coast United States, which can be higher than 20 ppbv [e.g., Brent *et al.*, 2015]. The first leg of the campaign, near the north eddy, was relatively clean, with less than 2 ppbv of NO₂ observed. Higher mixing ratios of NO₂, between 4 and 8 ppbv, were observed during the second leg of the campaign (7–9 August) because a cold front moving from the northwest brought a more terrestrial air mass over the study region. The NO₂ mixing ratios decreased to < 2 ppbv as the ship tracked toward the south eddy and the synoptic flows veered with time turning from northerly to southerly, bringing relatively clean marine air masses.

Surface O₃ was between 40 and 70 ppbv when at port, typical of terrestrial air masses in summer that have been impacted by photochemistry coupled with stable boundary layer conditions over a period of 2–3 days to elevate surface O₃ above background (~40 ppb) mixing ratios (Figure 2b). As the ship headed eastward to the north eddy during the first leg of the campaign, O₃ decreased to 25–35 ppbv (typical of background air) and remained near background until the ship returned to port on 5 August. The ship departed the port on 6 August at ~03:00 LST and headed eastward to the north eddy. On 6 August, the surface O₃ increased to 70 ppbv and remained elevated until 03:00 LST on 7 August when a cold front moving from the northwest cleared out residual, built-up O₃ at the surface and decreased the surface ozone to 55 ppbv. A steady decrease in surface O₃ mixing ratios was observed from 8 August to 13 August as the ship sampled near and south of the south eddy.

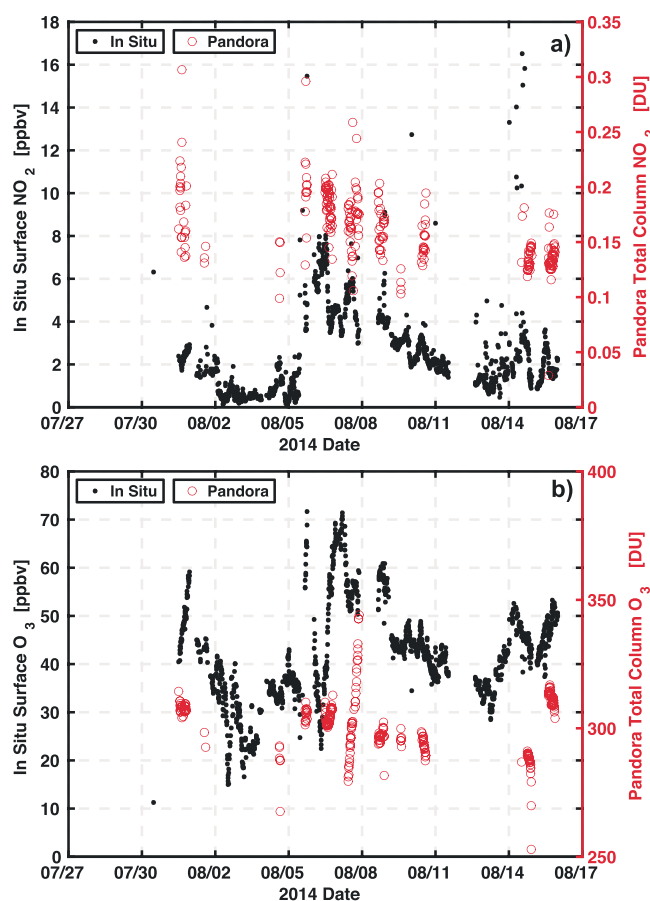


Figure 2. Time series of surface (black dots) and Pandora total column (red circles) (a) NO_2 and (b) O_3 .

local ship emissions. This hypothesis is supported by in situ surface NO_2 observations of >20 ppb at the time of the TCNO_2 measurement from Pandora. A diurnal cycle in TCNO_2 was not observed, as expected for open ocean environments away from urban nitric oxide emissions (Figure 3a).

As expected, these marine columns were relatively clean compared to NO_2 measured over ground-based sites near urban areas but are comparable to rural sites in the Chesapeake Bay watershed [Tzortziou *et al.*, 2015; Knepp *et al.*, 2015]. These measurements highlight the spatial heterogeneity of NO_x sources and chemistry that can dilute NO_2 in the total column downwind. The measured values of total column NO_2 provide evidence supporting the original hypothesis that there is a lack of spatial heterogeneity of NO_2 in the total column over this remote marine environments as well as comparing well with rural terrestrial environments. This result was expected but also highlights for the first time the good performance and precision of the ship-based Pandora under low pollution conditions.

The TCO_3 measurements from Pandora ranged between 283.4 and 343.0 DU with a median of 307.5 DU (Figure 2b). Intradiurnal variability of TCO_3 of up to 12 DU was observed, but no diurnal cycle was observed (Figure 3b). Higher TCO_3 s were observed near the north eddy compared to the south eddy and when

3.2. Ground-Based Spatial and Temporal Variability of TCNO_2 and TCO_3

The spatial and temporal variability of TCNO_2 and TCO_3 as measured by the Pandora were investigated during the sampling period (Table 1). TCNO_2 ranged from 0.04 to 0.57 DU with a median of 0.17 DU (Figure 2 a), similar to previous measurements along rural Atlantic coast sites [Tzortziou *et al.*, 2015]. The mean daily temporal average was 0.15 DU, and standard deviation was 0.03 DU. TCNO_2 measured above 0.3 DU on 3 days ($N=47$): 30 July, 5 August, and 15 August. Of these measurements, 74% were within 3 km of Lewes, DE. Back trajectory analyses showed that these measurements represent terrestrial air masses. The remaining measurements with $\text{TCNO}_2 > 0.3$ DU occurred within a 2 min time period on 15 August near the Atlantic continental shelf as the ship was tracking northwest toward the port. The limited duration of the TCNO_2 spike and the abundant ship activity along the continental shelf suggests that this spike was from

Table 1. Statistics of Total Column NO_2 and O_3 From Pandora On Board the *Hugh R. Sharp* for Measurements Collected Between 30 July and 15 August 2014

	Sample Points	Valid Sample Points	Minimum	Maximum	Median	Mean	Standard Deviation	Mean Uncertainty
	(#)	(#)	(DU)	(DU)	(DU)	(DU)	(DU)	(DU)
O_3	4867	3180	283.4	343.0	307.5	308.2	9.9	1.2
NO_2	4518	3793	0.04	0.57	0.17	0.17	0.04	0.01

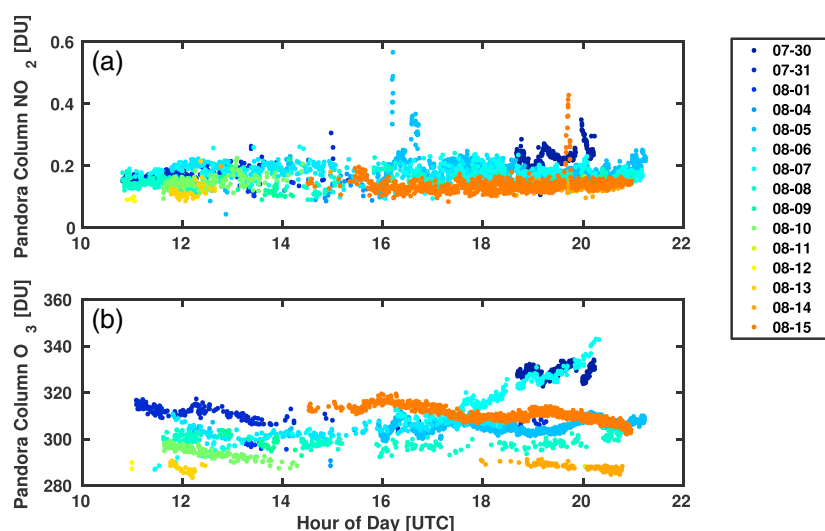


Figure 3. Diurnal time series of Pandora column measurements for (a) NO_2 and (b) O_3 . Each color represents a particular day of measurement during the campaign.

tracking to and from the port. The highest observed TCO₃ occurred on 7 August while sampling the north eddy, ~230 km from the east coast (Figure 1). On this day, the TCO₃ increased from 286.9 DU at 7:30 (LT) to 343.0 DU at 15:15 (LT). The ship tracked toward the south, covering 28 km during the Pandora sampling period on this day (38.0974 N; 72.3625 W). The highest marine surface O_3 of the campaign was observed on 7 August, but the surface O_3 decreased from 71 ppbv to 55 ppbv throughout the day, while TCO₃ was increasing. Given the minimal distance the ship traveled on this day, this observation suggests that plumes of elevated O_3 were advected over the ship. Since the total column O_3 theoretically would not change

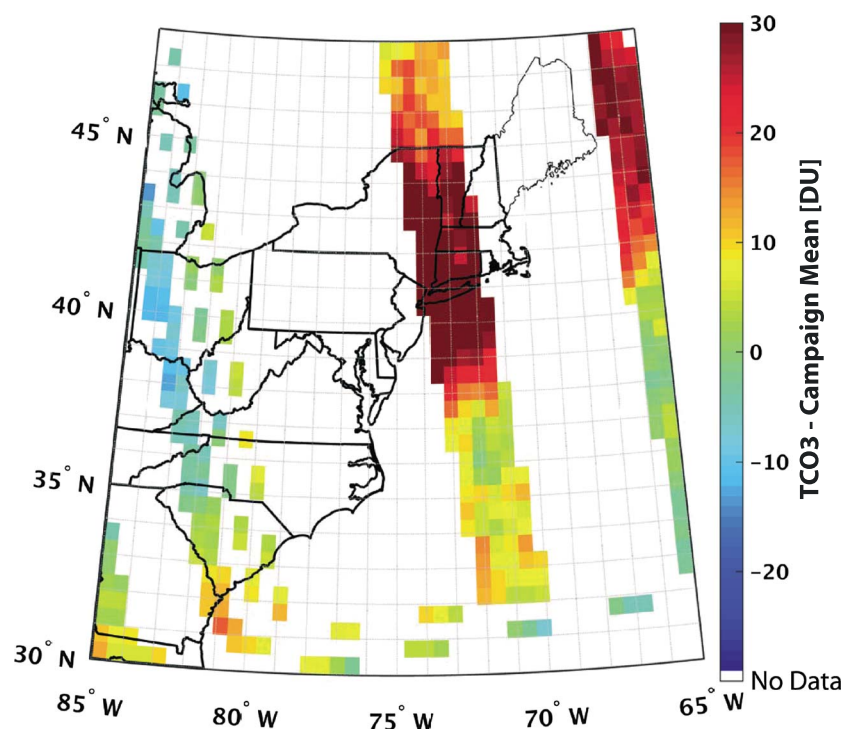


Figure 4. TCO₃ anomaly (daily, campaign mean) from OMI on 7 August 2014 18:34. The campaign mean includes data from all OMI overpasses between 20 July and 20 August 2014.

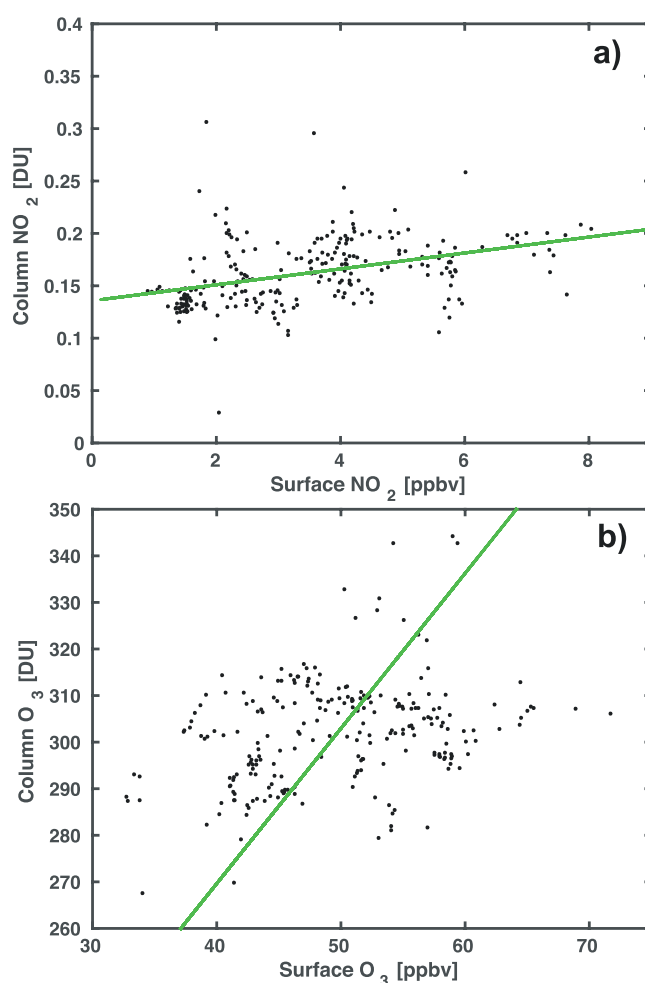


Figure 5. Correlations of Pandora total column to in situ surface mixing ratio measurements of (a) NO₂ and (b) O₃. The total least squares fit for each data set is shown (green line).

3.3. Pandora Comparison With In Situ Measurements

An orthogonal least squares regression to account for both errors in dependent and independent variables resulted in a slope of 0.008 ± 0.002 DU ppbv⁻¹ between 10 min averaged TCNO₂ and surface NO₂ mixing ratios (Figure 5a). The regression explained 99% of the observed variance. The observed correlation is smaller than previous terrestrial ground-based column versus in situ surface measurement of >0.75 [Knepp *et al.*, 2015]. However, given that the measurements discussed here are total column rather than tropospheric column and they are not located near major point source emissions, we expected lower correlations between column and surface measurements. If we assume that the surface measurement represents the average of the marine boundary layer, and the vertical profile of NO₂ mixing ratio in the marine boundary layer is constant, then the y intercept of the linear regression represents the TCNO₂ above the marine boundary layer, which is often considered as “background.” The assumption of a well-mixed marine boundary layer may be invalid but is needed to compare to results to previous work [Knepp *et al.*, 2015]. The y intercept of 0.136 DU TCNO₂ compares well with the lowest observed TCNO₂ from OMI averaged over the study period (Figure 6a).

An orthogonal least squares regression of TCO₃ against surface O₃ mixing ratios resulted in a slope of 3.33 ± 0.2 DU ppbv⁻¹. The regression explained 76% of the observed variance. The correlation is slightly smaller than the TCNO₂ to surface correlation presumably due to the vertical distributions of O₃ and NO₂ [e.g., Brent *et al.*, 2015]. Over the land, most of the tropospheric NO₂ is within the boundary layer since NO₂ is the product of combustion followed by rapid oxidation of nitric oxide. The vertical distribution of O₃ is more complex since it is a secondary pollutant formed by complex, nonlinear reactions with

due to tropopause folding or other stratospheric intrusions, we do not suspect that the observed increase is purely vertical dynamics in the upper atmosphere. Back trajectory analyses finishing at 8:00 (LT) show flow coming from the northwest at 500 and 2000 m and more westerly at 5000 m. As noted above, a weak cold front passed through the study region with an associated upper level low. Upper level lows typically induce shallow tropopause heights in which stratospheric air containing higher amounts of ozone are advected into the low center. This advection can cause increases in the TCO₃. OMI observations of TCO₃ show a north-south gradient (30–40 DU decrease) over the campaign mean over a distance of 5° of latitude, consistent with the Pandora temporal increase observed on 7 August as the terrestrial air mass advected southward (Figure 4). These results suggest that the large temporal change we observed in TCO₃ with Pandora on 7 August was potentially associated with stratospheric O₃ changes due to an upper level low pressure over this coastal area transporting air masses with higher TCO₃ over the area of the ship measurements.

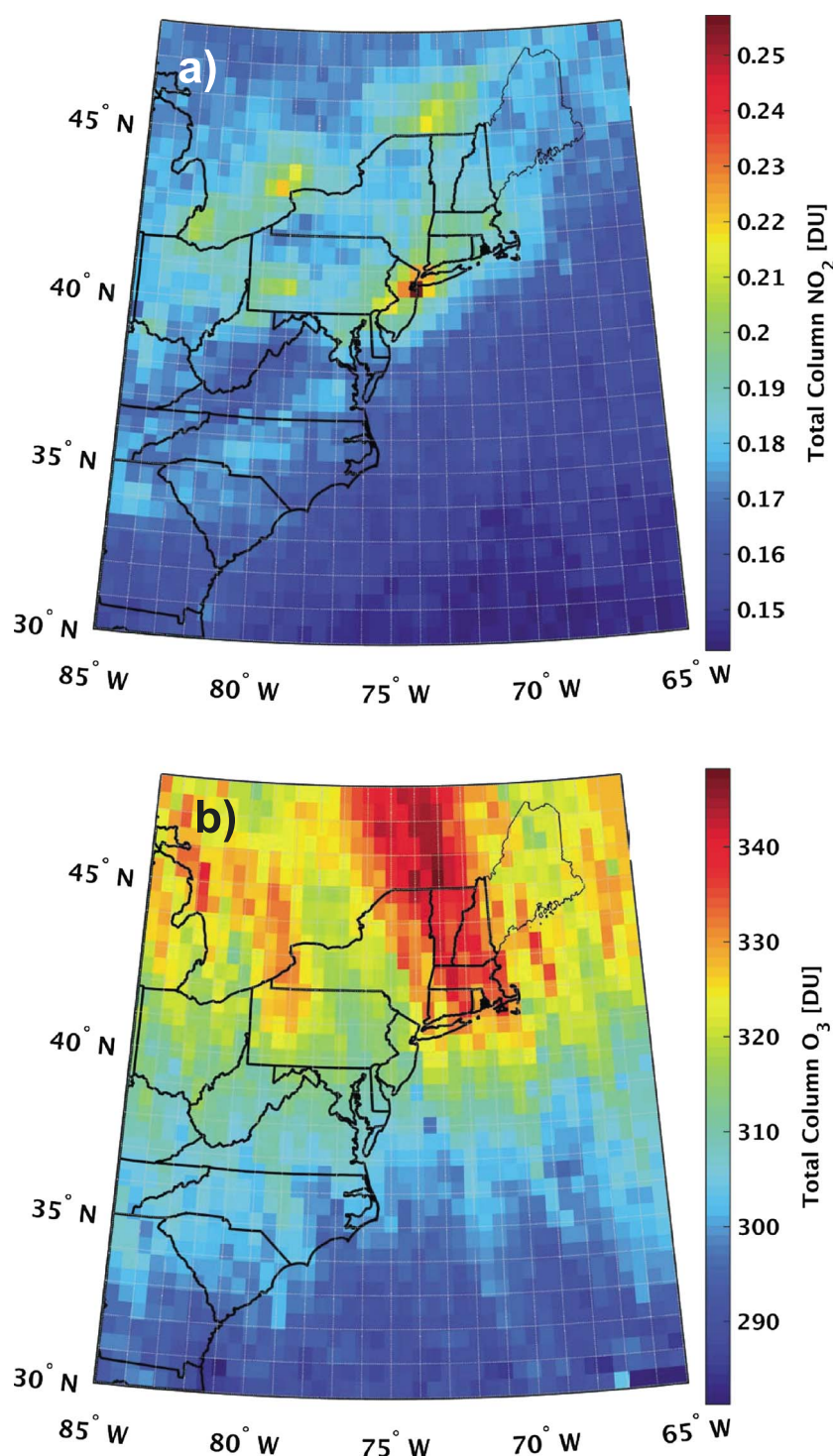


Figure 6. OMI total column averages of (a) NO₂ and (b) O₃ between 20 July and 20 August 2014.

NO_x and VOCs. Tropospheric and boundary layer ozone comprises only ~20% and 2–14%, respectively, of the total ozone column [Martins *et al.*, 2015]. The y intercept of the TCO₃ versus surface O₃ mixing ratio linear regression is 277 DU. This “background” TCO₃ is slightly lower than the lowest average value observed from OMI, but this result is expected given that the OMI average was from 20 July to 20 August 2014 when photochemical production is likely to occur in the Northern Hemisphere (Figure 6b).

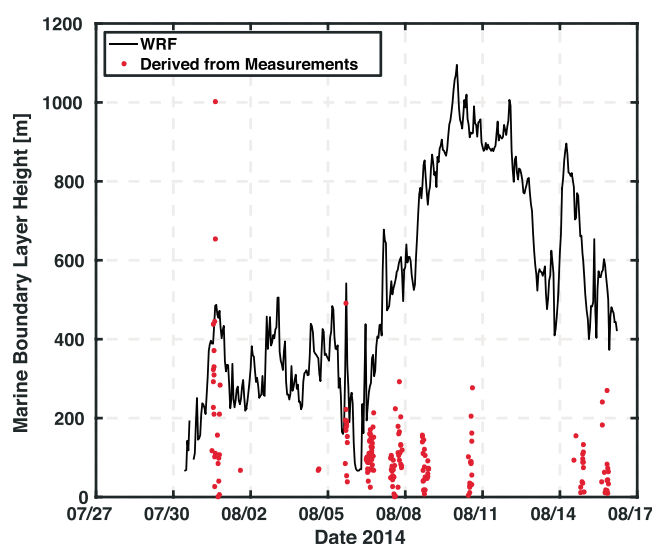


Figure 7. Modeled (black line) and derived (red dots) boundary layer heights.

From the NO_2 correlation analyses, we can derive a boundary layer height using [from Knepp *et al.*, 2015]

$$\text{TCNO}_2 = c\text{HN} + b \quad (1)$$

where TCNO_2 is the total column NO_2 from the Pandora in molecules cm^{-2} , c is the measured surface mixing ratio of NO_2 in $\text{mol}_{\text{NO}_2} \text{mol}_{\text{air}}^{-1}$, H is the marine boundary layer height, N is the average number density of air in the marine boundary layer in molecules cm^{-3} , and b is the y intercept of the correlation in molecules cm^{-2} . Here the slope, m , of the correlation plot is

$$m = \text{HN} \quad (2)$$

For this equation, it is assumed that most of the NO_2 resides in the boundary layer and that the planetary boundary layer (in this case the marine boundary layer) is well mixed. Solving equation (2) for boundary layer height using the regression coefficients of Figure 5 and an average temperature and pressure of 24.9°C and 1016.4 hPa, respectively, gives an average marine boundary layer height of 87 m. The boundary layer height, temperature, and pressure averages are the temporal average during the sampling period during which the Pandora measurements were valid, so it only comprises daytime measurements and the marine boundary layer height is an average daytime boundary layer height. There were little dependences (<20 m) of the calculated boundary layer heights on observed pressure and temperature based on a sensitivity test using the maximum and minimum pressures and temperatures in the calculation. This method of using the slope of the linear regression between column and surface measurements is not dependent on assumptions of column amount above the boundary layer.

The instantaneous boundary layer height was derived using 10 min averaged in situ surface, column measurements from Pandora, and a “background” column amount (i.e., column amount above the marine boundary layer (b , equation (1)) as 0.136 DU; Figure 7). Column measurements below this background, which would result in a negative boundary layer height, were not considered in this analysis. Average derived boundary layer heights ranged from 67 to 248 m with the intradiurnal variability of 69 m. Boundary layer heights were simulated using the Weather Research Forecasting (WRF) model with the Mellor-Yamada-Janjic (MYJ) [Mellor and Yamada, 1982; Janjic, 2002] boundary layer parameterization scheme, which has been shown to be the most reliable parameterization scheme in simulating marine atmospheric boundary layers [Krogsæter and Reuder, 2014]. The simulated boundary layer heights were higher than the derived boundary layer heights, with average daytime (8:00–18:00 LST) ranging from 157 to 950 m (Figure 7). The simulated boundary layer heights do not have a distinct diurnal cycle but are inversely proportional to latitude, suggesting that available energy at the surface within the model is driving the variability of the simulated boundary layer heights. Differences between the derived boundary layer height and the modeled boundary layer height are greater than those of previous studies comparing a variety of boundary layer height estimates

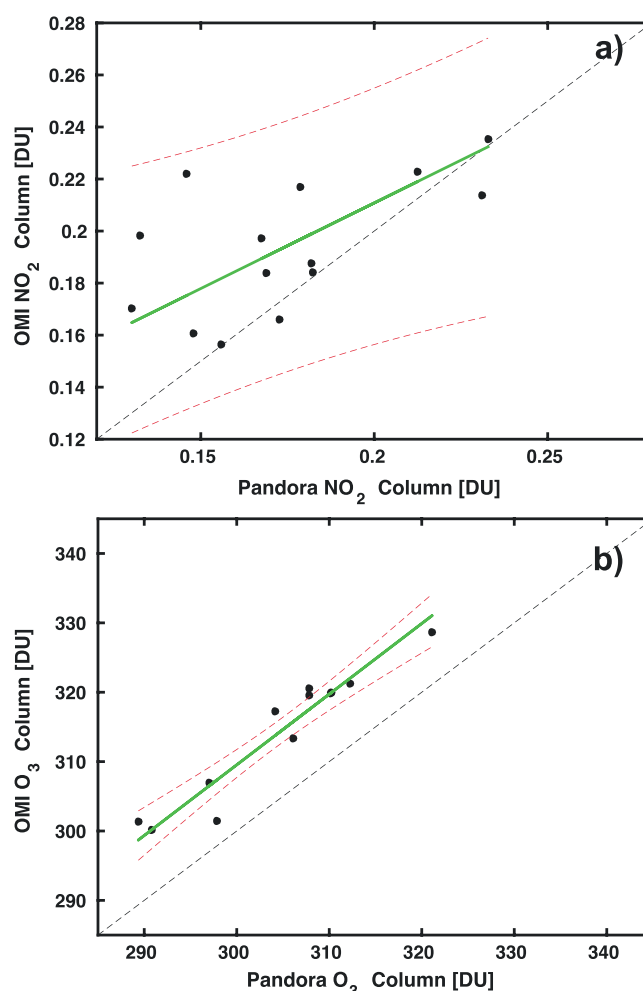


Figure 8. Comparison of concurrent OMI and Pandora total column (a) NO₂ and (b) O₃. A total least squares regression was fit to the data (green line), and 95% confidence limits (red dashed) and a 1:1 line are shown (black dashed).

[Knepp *et al.*, 2015; Kollonige *et al.*, submitted manuscript, 2015]. Satellite retrievals of boundary layer heights from the Atmospheric Infrared Sounder (AIRS), previously shown to be within 10% of radiosonde measurements (Kollonige *et al.*, submitted manuscript, 2015), have daily means of between 1059 m and 1998 m. These previous results, however, were collected over South Africa near large area sources of NO_x from the Johannesburg-Pretoria megacity. The AIRS boundary layer height retrievals are higher than the derived boundary layer heights from equation (2) from the WRF simulations. These differences suggest either (1) the assumptions of a constant NO₂ column above the boundary layer and/or that the surface mixing ratio measurement is representative of the stable marine boundary layer are not valid or (2) the mixing and/or turbulence (both mechanical and buoyant) are overestimated in the model. The disagreements of these results with previous work over terrestrial environments highlight the need for additional data over marine environments to validate these methods and the assumptions behind them. These analyses show the utility of having colocated surface and column measurements to infer the dynamics of the atmosphere and vertical distribution of the pollutant. Satellites rely on prior NO₂ profile shapes, which typically come from monthly averaged model simulations, to retrieve NO₂ column amounts. The NO₂ profile shapes are dependent on proximity to point sources, photochemistry, and vertical mixing; the latter can be characterized using an estimate of marine boundary layer height. The coarse model resolution of the 2° × 2.5° Global Modeling Initiative (GMI), the simulations used for the monthly mean a priori NO₂ profiles, can be a significant source of error of the retrieved NO₂ columns [Lamsal *et al.*, 2014]. However, evaluating the GMI NO₂ profile shapes over marine environments is beyond the scope of this work.

Table 2. Comparison Statistics of OMI and the Ship Pandora Coincident and Colocated Total Column Measurements of NO₂ and O₃^a

	Number of Samples (#)	Mean Bias (OMI-Pandora) (DU)	Percent Bias (%)	RMSE (DU)	NRMSE (%)	Slope (OMI/Pandora)	Explained Variance of Total Least Squares Fit (%)
O ₃	12	9.6 ± 1.4	3.2	10.0	3.2	1.02	98.0
NO ₂	14	0.02 ± 0.01	11.5	0.03	16.8	0.66	81.1

^aCoincidence is defined as within 60 min and 300 km of each measurement.

3.4. OMI and Pandora Comparison

Total column NO₂ and O₃ retrievals from Pandora were compared with colocated and coincident OMI overpass total column NO₂ and O₃. Because OMI only overpasses a particular point on Earth's surface once per day around solar noon and clouds can interfere with both ground- and satellite-based retrievals, 14 concurrent OMI and Pandora measurements for NO₂ and 12 for O₃ were collected during the 16 day campaign. Each day during the sampling period, the average position of the ship was calculated. The OMI swath data that were within 300 km of the ship's position were used to calculate the average overpass time of the satellite. Two overpasses were used on 8 days, occurring when the ship was on the western side of the swath during the earlier overpass and on the eastern side of the swath during the later overpass. On average, the later overpass occurred 98 min after the earlier overpass, consistent with the orbital period of the Aura satellite. In this case, each overpass was averaged and compared to coincident Pandora data separately. Pandora data within 1 h of the satellite overpass(es) were averaged, and the mean locations of those data were calculated. Column data from OMI within 300 km of the mean Pandora location were averaged and compared to Pandora measurements.

Differences between OMI and Pandora TCNO₂ ranged from −0.02 to 0.08 DU. A total least squares fit resulted in a slope of 0.66, explaining 81.1% of the variance (Figure 8a). A mean bias for TCNO₂ of 0.02 DU (11.5%) and root-mean-square error (RMSE) of 0.03 DU (16.8%) compared to OMI was observed (Table 2). In all but one concurrent pair, OMI overestimated the Pandora measurements, especially at the lower NO₂ amounts (Figure 8a). This result is consistent with previous results showing that OMI on average overestimated TCNO₂ at rural sites [Tzortziou *et al.*, 2015]. However, OMI significantly underestimates TCNO₂ in areas impacted by strong (local or long-range transport) pollution, showing a mean bias of −15.5% compared to Pandora measurements impacted by anthropogenic emissions [Reed *et al.*, 2015; Tzortziou *et al.*, 2015]. These previous studies show that the ground-based Pandora measurements are more sensitive to the spatial heterogeneity of surface emissions compared to satellite measurements. The relatively clean observations in this study show that the measurements are not being impacted by local emissions or boundary layer spatial and/or temporal variability.

Differences between OMI and Pandora TCO₃ ranged from 3.6 to 13.0 DU. A total least squares fit resulted in a slope of 1.02, explaining 98.0% of the variance (Figure 8b). A mean bias of 9.6 DU (3.2%) and RMSE of 10.0 DU (3.2%) was observed (Table 2) with OMI systematically overestimating TCO₃ compared to Pandora, consistent with previous studies [Reed *et al.*, 2015; Tzortziou *et al.*, 2015].

4. Conclusion

Total column and surface measurements of NO₂ and O₃ as part of the DANCE campaign during the summer of 2014 in the North Atlantic Ocean show relatively clean air masses compared to terrestrial air masses. A pollution episode was observed on 7 August 2014, which brought air from New England. Mixing ratios of 7 ppbv and 70 ppbv of NO₂ and O₃ were observed during the pollution episode. Statistically significant correlations were observed between the NO₂ and O₃ total column measurements and the respective in situ surface measurements over the entire campaign.

An evaluation and comparison of satellite total column NO₂ and O₃ from the OMI instrument onboard the Aura satellite and Pandora measurements show similar correlations and biases compared to previous terrestrial studies [Tzortziou *et al.*, 2015]. This work, while spatially and temporally limited, has provided the first open-water evaluation of TCNO₂ and TCO₃ from OMI using the shipboard Pandora instrument. Further evaluations need to be conducted to understand how terrestrial air masses influence the vertical distribution of

pollutants in and above the stable marine boundary layer as well as impact the satellite and ground-based remote sensors. More observations of NO₂ and O₃ surface mixing ratios and total columns, as well as boundary layer height, are needed to evaluate models that are used in satellite retrievals and as initial and boundary conditions for other regional models.

Acknowledgments

This work was funded by the National Science Foundation Division of Ocean Sciences (1260574), NASA's DISCOVER-AQ (NNX10AR39G), AQAAT (NNXAQ44G), and NASA's Pandora work (NNX13AL86G). We thank the captain and the crew of the R/V *Hugh R. Sharp*. We thank James Szykman and Winston Luke for their collaborations. The authors gratefully acknowledge the NOAA Air Resources Laboratory (ARL) for the provision of the HYSPLIT transport and dispersion model and/or READY website (<http://www.ready.noaa.gov>) used in this publication. For data access, please contact the project Principal Investigator Raymond Najjar, rgn1@psu.edu.

References

- Boersma, K. F., et al. (2007), Near-real time retrieval of tropospheric NO₂ from OMI, *Atmos. Chem. Phys.*, **7**, 2103–2118.
- Boersma, K. F., et al. (2008), Validation of OMI tropospheric NO₂ observations during INTEX-B and application to constrain NO_x emissions over the eastern United States and Mexico, *Atmos. Environ.*, **42**(19), 4480–4497, doi:10.1016/j.atmosenv.2008.02.004.
- Brent, L. C., et al. (2015), Evaluation of the use of a commercially available cavity ringdown absorption spectrometer for measuring NO₂ in flight, and observations over the Mid-Atlantic States, during DISCOVER-AQ, *J. Atmos. Chem.*, **72**(3–4), 503–521, doi:10.1007/s10874-013-9265-6.
- Bucsela, E. J., N. A. Krotkov, E. A. Celarier, L. N. Lamsal, W. H. Swartz, P. K. Bhartia, K. F. Boersma, J. P. Veefkind, J. F. Gleason, and K. E. Pickering (2013), A new stratospheric and tropospheric NO₂ retrieval algorithm for nadir-viewing satellite instruments: Applications to OMI, *Atmos. Meas. Tech.*, **6**(10), 2607–2626.
- Cede, A., J. Herman, A. Richter, N. Krotkov, and J. Burrows (2006), Measurements of nitrogen dioxide total column amounts using a Brewer double spectrophotometer in direct Sun mode, *J. Geophys. Res.*, **111**, D05304, doi:10.1029/2005JD006585.
- Duncan, B. N., L. N. Lamsal, A. M. Thompson, Y. Yashido, Z. Lu, D. G. Streets, M. M. Hurwitz, and K. E. Pickering (2016), A space-based, high-resolution view of notable changes in urban NO_x pollution around the world (2005–2014), *J. Geophys. Res. Atmos.*, **121**, 976–996, doi:10.1002/2015JD024121.
- Fishman, J., et al. (2008), Remote sensing of tropospheric pollution from space, *Bull. Am. Meteorol. Soc.*, **805**–821.
- Herman, J., A. Cede, E. Spinei, G. Mount, M. Tzortziou, and N. Abuhassan (2009), NO₂ column amounts from ground-based Pandora and MDOAS spectrometers using the direct-Sun DOAS technique: Intercomparisons and application to OMI validation, *J. Geophys. Res.*, **114**, D13307, doi:10.1029/2009JD011848.
- Janjic, Z. I. (2002), Nonsingular implementation of the Mellor-Yamada level 2.5 scheme in the NCEP Meso model. NCEP Office Note 437, 61 pp.
- Knepp, T., et al. (2015), Estimating surface NO₂ and SO₂ mixing ratios from fast-response total column observations and potential application to geostationary missions, *J. Atmos. Chem.*, **72**(3–4), 261–286, doi:10.1007/s10874-013-9257-6.
- Krogsaeter, O., and J. Reuder (2014), Validation of boundary layer parameterization schemes in the Weather Research and Forecasting (WRF) model under the aspect of offshore wind energy applications-part II: Boundary layer height and atmospheric stability, *Wind Energy*, **18**, 1291–1302.
- Lamsal, L. N., et al. (2014), Evaluation of OMI operational standard NO₂ column retrievals using in situ and surface-based NO₂ observations, *Atmos. Chem. Phys.*, **14**, 11,587–11,609, doi:10.5194/acp-14-11587-2014.
- Martins, D. K., R. M. Stauffer, A. M. Thompson, H. S. Halliday, D. Kollonige, E. Joseph, and A. J. Weinheimer (2015), Ozone correlations between mid-tropospheric partial columns and the near-surface at two mid-Atlantic sites during the DISCOVER-AQ campaign in July 2011, *J. Atmos. Chem.*, **72**(3), 373–391.
- McPeters, R., M. Kroon, G. Labow, E. Brinksma, D. Balis, I. Petropavlovskikh, J. P. Veefkind, P. K. Bhartia, and P. F. Levelt (2008), Validation of the Aura Ozone Monitoring Instrument total column ozone product, *J. Geophys. Res.*, **113**, D15S14, doi:10.1029/2007JD008802.
- Mellor, G. L., and T. Yamada (1982), Development of a turbulence closure model for geophysical fluid problems, *Rev. Geophys. Space Phys.*, **20**, 851–875.
- National Research Council (2008), *Earth Observations From Space: The First 50 Years of Scientific Achievements*, 129 pp., Natl. Acad. Press, Washington, D. C.
- Osterman, G. B., et al. (2008), Validation of Tropospheric Emission Spectrometer (TES) measurements of the total, stratospheric, and tropospheric column abundance of ozone, *J. Geophys. Res.*, **113**, D15S16, doi:10.1029/2007JD008801.
- Platt, U., and J. Stutz (2008), *Differential Optical Absorption Spectroscopy: Principles and Applications*, 597 pp., Springer, Verlag, Heidelberg.
- Reay, D. S., F. Dentener, P. Smith, J. Grace, and R. A. Feely (2008), Global nitrogen deposition and carbon sinks, *Nat. Geosci.*, **1**, 430–437.
- Reed, A. J., A. M. Thompson, D. E. Kollonige, D. K. Martins, M. A. Tzortziou, J. R. Herman, T. A. Berkoff, N. K. Abuhassan, and A. Cede (2015), Effects of local meteorology and aerosols on ozone and nitrogen dioxide retrievals from OMI and Pandora spectrometers in Maryland, USA during DISCOVER-AQ 2011, *J. Atmos. Chem.*, **72**(3–4), 455–482, doi:10.1007/s10874-013-9254-9.
- Stein, A. F., R. R. Draxler, G. D. Rolph, B. J. B. Stunder, M. D. Cohen, and F. Ngan (2015), NOAA's HYSPLIT atmospheric transport and dispersion modeling system, *Bull. Am. Meteorol. Soc.*, **96**(12), 2059–2077.
- Tzortziou, M., J. R. Herman, A. Cede, and N. Abuhassan (2012), High precision, absolute total column ozone measurements from the Pandora spectrometer system: Comparisons with data from a Brewer double monochromator and Aura OMI, *J. Geophys. Res.*, **117**, D16303, doi:10.1029/2012JD017814.
- Tzortziou, M., J. R. Herman, Z. Ahmad, C. P. Loughner, N. Abuhassan, and A. Cede (2014), Atmospheric NO₂ dynamics and impact on ocean color retrievals in urban nearshore regions, *J. Geophys. Res. Oceans*, **119**, 3834–3854, doi:10.1002/2014JC009803.
- Tzortziou, M., J. R. Herman, A. Cede, C. P. Loughner, N. Abuhassan, and S. Naik (2015), Spatial and temporal variability of ozone and nitrogen dioxide over a major urban estuarine ecosystem, *J. Atmos. Chem.*, **72**(3–4), 287–309, doi:10.1007/s10874-013-9255-8.
- United States Environmental Protection Agency (2012), *Our Nation's Air: Status and Trends Through 2010*, Research Triangle Park, NC, EPA-454/R-12-001.
- Velders, G. J. M., C. Granier, R. W. Portmann, K. Pfeilsticker, M. Wenig, T. Wagner, U. Platt, A. Richter, and J. P. Burrows (2001), Global tropospheric NO₂ column distributions: Comparing three-dimensional model calculations with GOME measurements, *J. Geophys. Res.*, **106**(D12), 12,643–12,660, doi:10.1029/2000JD900762.